Journal of Virology®

CELLULAR RESPONSE TO INFECTION

IRF2 Cooperates with Phosphoprotein of Spring Viremia of Carp Virus to Suppress Antiviral Response in Zebrafish

Wenji Huang,[a,b,c] Xin Zhao,[a,b,c] Ning Ji,[a,b,c] Jiahong Guo,[a,b,c] Jianhua Feng,[a,b,c] Kangyong Chen,[a,b,c] Yaxin Wu,[a,b,c] Junya Wang,[a,b,c] Hao Feng,[d] Jun Zou[a,b,c,e]

[a]Key Laboratory of Exploration and Utilization of Aquatic Genetic Resources, Ministry of Education, Shanghai Ocean University, Shanghai, China
[b]International Research Center for Marine Biosciences, Ministry of Science and Technology, Shanghai Ocean University, Shanghai, China
[c]National Demonstration Center for Experimental Fisheries Science Education, Shanghai Ocean University, Shanghai, China
[d]State Key Laboratory of Developmental Biology of Freshwater Fish, College of Life Science, Hunan Normal University, Changsha, China
[e]Laboratory for Marine Biology and Biotechnology, Qingdao National Laboratory for Marine Science and Technology, Qingdao, China

Wenji Huang and Xin Zhao contributed equally to this work. Author order was determined in order of decreasing seniority.

ABSTRACT IFN regulatory factor (IRF) 2 belongs to the IRF1 subfamily, and its functions are not yet fully understood. In this study, we showed that IRF2a was a negative regulator of the interferon (IFN) response induced by spring viremia of carp virus (SVCV). *Irf2a*$^{-/-}$ knockout zebrafish were less susceptible to SVCV than wild-type fish. Transcriptomic analysis reveals that differentially expressed genes (DEGs) in the *irf2a*$^{-/-}$ and *irf2a*$^{+/+}$ cells derived caudal fins were mainly involved in cytokine-cytokine receptor interaction, mitogen-activated protein kinase (MAPK) signaling pathway, and transforming growth factor-beta (TGF-beta) signaling pathway. Interestingly, the basal expression levels of interferon stimulating genes (ISGs), including *pkz*, *mx*, *apol*, and *stat1* were higher in the *irf2a*$^{-/-}$ cells than *irf2a*$^{+/+}$ cells, suggesting that they may contribute to the increased viral resistance of the *irf2a*$^{-/-}$ cells. Overexpression of IRF2a inhibited the activation of *ifn*φ*1* and *ifn*φ*3* induced by SVCV and poly(I:C) in the epithelioma papulosum cyprini (EPC) cells. Further, it was found that SVCV phosphoprotein (SVCV-P) could interact with IRF2a to promote IRF2a nuclear translocation and protein stability via suppressing K48-linked ubiquitination of IRF2a. Both IRF2a and SVCV-P not only destabilized STAT1a but reduced its translocation into the nucleus. Our work demonstrates that IRF2a cooperates with SVCV-P to suppress host antiviral response against viral infection in zebrafish.

IMPORTANCE Interferon regulatory factors (IRFs) are central in the regulation of interferon-mediated antiviral immunity. Here, we reported that IRF2a suppressed interferon response and promoted virus replication in zebrafish. The suppressive effects were enhanced by the phosphoprotein of the spring viremia of carp virus (SVCV) via inhibition of K48-linked ubiquitination of IRF2a. IRF2a and SVCV phosphoprotein cooperated to degrade STAT1 and block its nuclear translocation. Our work demonstrated that IRFs and STATs were targeted by the virus through posttranslational modifications to repress interferon-mediated antiviral response in lower vertebrates.

KEYWORDS IRF2a, SVCV, STAT1a, ubiquitination, antiviral response, interferon regulatory factor, interferon signaling

Interferon-regulatory factors (IRFs) belong to a family of evolutionarily conserved transcription factors which regulate the production of type I interferons (IFNs) and host antiviral responses (1). Nine IRFs are found in humans and 11 in fish with IRF10 identified only in birds and teleost fish (2). All IRFs contain a conserved N-terminal DNA-binding domain (DBD), which recognizes DNA motifs similar to the IFN-stimulated response

Editor Bryan R.G. Williams, Hudson Institute of Medical Research

Address correspondence to Jun Zou, jzou@shou.edu.cn.

The authors declare no conflict of interest.

Received 25 August 2022
Accepted 8 October 2022
Published 31 October 2022

element (ISRE), and a C-terminal region harboring an IRF-associated domain (IAD), which is responsible for the regulation of IRF activities. Most IRFs contain an IAD1 except for IRF1 and IRF2, which possess an IAD2 instead. Based on the IAD domain, IRFs can be grouped into four subfamilies, namely, IRF1 (IRF1, 2 and 11), IRF3 (IRF3 and 7), IRF4 (IRF4, 8, 9, and 10), and IRF5 (IRF5 and 6) (1–3).

Interferon-regulatory factors are widely involved in the signaling events of pattern recognition receptors (PRRs) activated by pathogen-associated molecular patterns (PAMPs). Several studies have shown that IRF1, IRF3, IRF7, and IRF9 serve as positive regulators of the IFN response (4, 5). The deficiency of these IRFs in mammals increases the susceptibility of the host to pathogens, particularly viruses. For instance, IRF3 and IRF7 knockout mice exhibit increased viral load after influenza A infection (6), while IRF1 is required for the restriction of vesicular stomatitis virus, influenza virus, dengue virus, and other dsRNA viruses (7–9). However, although the functions of most IRFs are known, IRF2 has been poorly investigated. Existing evidence demonstrates that IRF2 decreases the IFN-triggered transcriptional expression of ISGs, and IRF2 deficiency decreases mortality caused by lymphocytic choriomeningitis virus infection (10). Furthermore, overexpression of IRF2 leads to a severe infection with West Nile Virus (11), while negatively regulating neurovirus invasion and replication (12). IRF2 can be SUMOylated *in vivo* by PIASy and cooperates with transcription factors such as RelA and signal transducer and activator of transcription 1 (STAT1) to regulate signaling pathways (13–15).

Viruses have evolved strategies to manipulate host factors to counteract immune defense. Factors involved in the IFN pathway are the prime targets exploited by viruses. For instance, Zika virus NS5 impairs retinoic acid-inducible gene (RIG)-I polyubiquitination and attenuates phosphorylation and nuclear translocation of IRF3, blocking RIG-I-activated signal transduction (16). Moreover, influenza A virus NS1 targets ubiquitin ligases, such as tripartite motif-containing protein 25 (TRIM25) to escape recognition by PRRs (17). Rabies virus phosphoprotein interacts directly with STAT1 through the C-terminal domain to inhibit the translocation of phosphorylated STAT1 into the nucleus to suppress the IFN-stimulated Janus kinase/signal transducers and activators of transcription (JAK-STAT) signaling (18, 19).

Spring viremia of carp virus (SVCV) is a negative-stranded ssRNA virus that belongs to the genus *Vesiculovirus* of the family *Rhabdoviridae*. It infects a range of cyprinid fishes, including zebrafish, and has been widely used to study host and pathogen interaction. Previous studies have shown that SVCV phosphoprotein (SVCV-P) is actively involved in counteracting host antiviral defenses by competing with host IRF3 to bind to TBK1, resulting in decreased phosphorylation of IRF3 (20). Besides, SVCV nucleoprotein (SVCV-N) promotes the degradation of MAVS (21). In this study, we analyzed transcriptomic profiles of *irf2a*$^{-/-}$ zebrafish in response to SVCV infection and identified IRF2a as a negative regulator in IFN-mediated antiviral immunity. Both IRF2a and SVCV-P suppressed STAT1a activity by blocking its nuclear translocation. Furthermore, we found that SVCV-P protein could stabilize IRF2a protein by impairing K48-linked ubiquitination and increasing its nuclear translocation. Our findings revealed a complex regulatory mechanism that governed the interactions between host IRFs and viruses via posttranslational modifications.

RESULTS

IRF2a negatively regulated IFN response and promoted viral replication. To elucidate more fully the function of IRF2, we overexpressed IRF2a in the primary caudal fin cells from WT fish and examined the expression of antiviral genes after SVCV infection. We found that overexpression of IRF2a repressed the expression of *ifnφ1* and *mx1* but, surprisingly, not *pkr* and *isg15* at 24 h after infection (Fig. 1A). Consistent with this, the expression levels of *svcv-n* and *svcv-g* genes were elevated, and the virus titer of IRF2a-overexpressed cells was significantly higher than that of the control cells (Fig. 1B and C). Together, the results illustrated that zebrafish IRF2a suppressed the host antiviral response to promote viral replication. To determine the functional domains

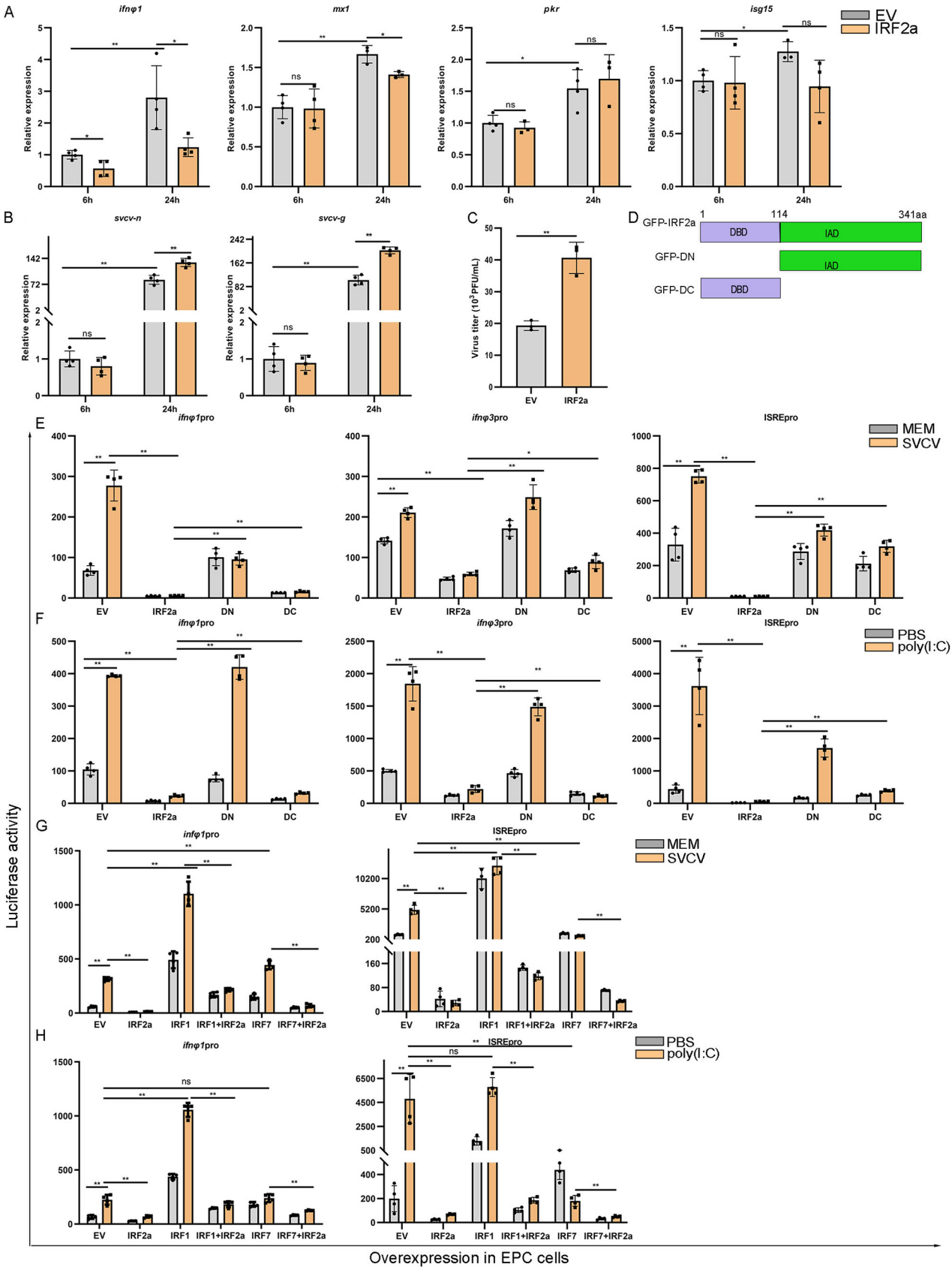

FIG 1 Overexpression of IRF2a suppressed IFN production and promoted SVCV replication. (A and B) The caudal fin cells derived from wild-type (WT) adult zebrafish were seeded in 6-well plates overnight and transfected with pEGFP-IRF2a (2 μg) or pEGFP-N1 (EV) (2 μg) for 24 h.

(Continued on next page)

that were responsible for suppressing the immune response, we generated domain-mutated IRF2a constructs (Fig. 1D) and found that overexpression of the IRF2a mutant DN (lacking the N-terminal DBD) rescued the promoter activities of *ifnφ1*, *ifnφ3* and ISRE compared to full-length IRF2a, while the IRF2a mutant DC (lacking the C-terminal IAD) still decreased the activity of gene promoters (Fig. 1E and F). It has been well-documented that DBD recognizes DNA motifs and IAD regulates IRF functions (3). Our results indicated that DBD, but not IAD, was required for the regulatory activity of IRF2a. Interestingly, overexpression of IRF2a and either IRF1 or IRF7 also decreased the activity of *ifnφ1* and ISRE promoters, suggesting that IRF2a acted as a suppressor for IRF1/IRF7-activated IFN production (Fig. 1G and H).

The *irf2a*$^{-/-}$ cells exhibited enhanced resistance to virus infection. Having shown that IRF2a negatively regulated the IFN response, we generated *irf2a* knockout zebrafish to further investigate the roles of IRF2a in the immune response to viral infection. We found that *irf2a*$^{-/-}$ larvae had a higher survival rate than the *irf2a*$^{+/+}$ larvae after infection with SVCV (Fig. 2A). Furthermore, antiviral genes such as *ifnφ1*, *mda5a*, and *mx1* were induced (Fig. 2B). Next, we prepared the cell cultures from the caudal fin of *irf2a*$^{+/+}$ and *irf2a*$^{-/-}$ fish and evaluated their susceptibility to viral infection. We observed that compared to the *irf2a*$^{+/+}$ cells, the *irf2a*$^{-/-}$ cells exhibited a sharp decrease in the number of viruses released to the medium and reduced expression levels of *svcv-n* and *svcv-g* genes (Fig. 2C and D). Further, the expression levels of genes involved in the IFN pathways, such as *ifnφ1*, *mx1*, and *isg15*, were relatively higher, indicating that the IFN response was more pronounced in the *irf2a*$^{-/-}$ cells than *irf2a*$^{+/+}$ cells (Fig. 2E). It must be noted that the expression levels of *ifnφ3* and *pkr* remained unchanged (Fig. 2E). Next, we performed RNA-seq to identify differentially expressed genes (DEGs) and identified 11,623 DEGs. To obtain the profiles of interrelationships in the four groups, the correlation of samples was analyzed using the principal component analysis (PCA), revealing that two distinct well-clustered groups were observed for the *irf2a*$^{+/+}$ and *irf2a*$^{-/-}$ cells. The patterns of the gene expression in the *irf2a*$^{+/+}$ and *irf2a*$^{-/-}$ cells had a 76.8% difference (Fig. 2F). Gene set enrichment analysis (GSEA) for DEGs in *irf2a*$^{-/-}$ cells compared with *irf2a*$^{+/+}$ cells revealed that the major pathways mediating antiviral response, including the cytokine-cytokine receptor interaction, MAPK signaling pathway, and TGF-beta signaling pathway were enriched (Fig. 2G to I). A previous study has identified 360 antiviral effector ISGs limiting virus replication, packaging, and release, including *mx*, *ifit*, *rsad2*, and chemokine genes (22), and some genes such as *ifnφ1*, *irf3*, *mx*, *pmsb8a* and *pmsb9a* with relatively higher expression levels could be detected in the *irf2a*$^{-/-}$ cells (Fig. 2J and K). These results prompted us to hypothesize that IRF2a may act as a suppressor of host antiviral response.

IRF2a regulated *pim* genes to promote SVCV replication. Serine/threonine kinases (STPK) regulate a variety of cellular processes such as the innate immune response to bacterial and viral infection and apoptosis (23). Previous studies have shown that *pim* family genes were markedly induced after SVCV infection (24). In our RNA-seq analysis, we observed that most of the STPK genes, including *pim*, *mknk2b*, *stk*, and *cdk* genes, were downregulated in the *irf2a*$^{-/-}$ cells (Fig. 3A). The *pim* genes were significantly upregulated in the *irf2a*$^{+/+}$ cells infected with SVCV, but the induced expression was mitigated in the *irf2a*$^{-/-}$ cells (Fig. 3B). We selected *pim1*, *pim2*, and *pim3* to verify the expression in the *irf2a*$^{+/+}$ and *irf2a*$^{-/-}$ cells by quantitative real-time PCR (qRT-PCR) analysis. Consistent with the RNA-seq analysis, the induced expression of the *pim1* gene reduced from 1.3-fold to 0.8-fold, the *pim2* gene decreased from 26-

FIG 1 Legend (Continued)
The cells were infected with SVCV (multiplicity of infection [MOI] = 1 for 24 h). Gene expression of host immune genes (A) and viral genes (B) was analyzed by qRT-PCR. (C) Viral titers of the culture medium collected from the above-described experiment (B) were measured by plaque assay (n = 3). (D) Diagram of wild-type IRF2a and two mutants lacking the N-terminal DBD (DN) and lacking the C-terminal IAD (DC). (E and F) EPC cells were transfected with 250 ng of *ifnφ1*pro-Luc, *ifnφ3*pro-Luc, or ISREpro-Luc plus pRL-TK (25 ng) plus 250 ng of pEGFP-IRF2a, pEGFP-IRF2a-DN, pEGFP-IRF2a-DC or pEGFP-N1 (EV). At 24 h posttransfection, cells were infected with SVCV (MOI = 1) or transfected with poly(I:C) (5 μg/mL) (F). (G and H) EPC cells were transfected with either pEGFP-IRF2a (250 ng), IRF1 (250 ng), or IRF7 (250 ng) plasmids for promoter analysis as described above. Transfected EPC cells were infected with SVCV (MOI = 1) (G) or transfected with poly(I:C) (5 μg/mL) (H). Gene expression was determined by qRT-PCR. *, $P < 0.05$; **, $P < 0.01$ were considered significant (n = 4).

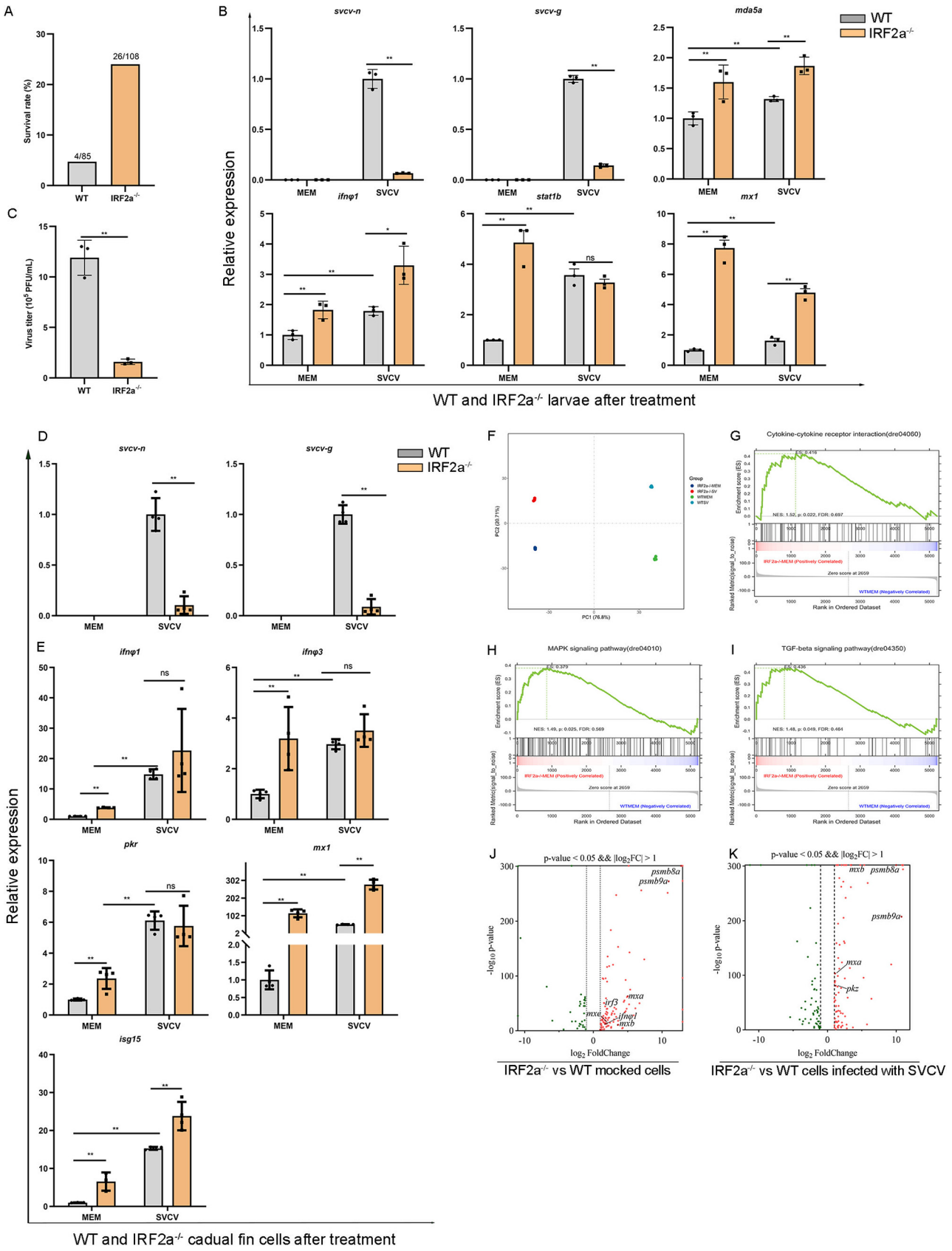

FIG 2 The *irf2a*$^{-/-}$ zebrafish and derived caudal fin cells exhibit enhanced resistance to SVCV infection. (A and B) The *irf2a*$^{+/+}$ and *irf2a*$^{-/-}$ larvae (5 dpf) were infected by immersion challenge for 12 h. The survival rate was recorded after 44 h (A) and gene expression was analyzed by qRT-

(Continued on next page)

fold to 6-fold, and that of the *pim3* gene from 2.2-fold to 1.4-fold in the *irf2a*$^{-/-}$ cells relative to the *irf2a*$^{+/+}$ cells after SVCV infection (Fig. 3C). Next, we overexpressed *pim* genes in the EPC cells and found that the transcript levels of the *svcv-g* and *svcv-n* genes were significantly higher in the cells transfected with *pim2* and *pim3* genes than in those with vector plasmids (Fig. 3D). In line with the gene expression data, virus titers were considerably higher in the *pim2* and *pim3* transfected cells than in the mock-transfected cells (Fig. 3E). However, the cells transfected with the *pim1* gene displayed decreased transcript levels of *svcv-g* and *svcv-n* relative to the mock-transfected cells. The virus titers of the cells transfected with empty vectors, *pim1*, *pim2*, and *pim3* were 10.8×10^3, 7.1×10^3, 126.6×10^3, and 78.3×10^3 PFU/mL, respectively (Fig. 3E). To further explore the regulation of the PIM kinases and IRF2a in viral replication, we pretreated *irf2a*$^{+/+}$ cells with pan-PIM kinase inhibitor (PIM447) for 10 h and infected the cells with SVCV for 24 h. We observed that the expression of *svcv-n* and *svcv-g* and virus titers were markedly reduced in *irf2a* overexpressed cells after exposure to PIM447 (Fig. 3F and G). These results demonstrate that IRF2a is involved in the regulation of the PIM-mediated response to virus infection.

SVCV-P promoted nuclear translocation and stability of IRF2a. Given that overexpression of *irf2a* enhanced viral replication in the *irf2a*$^{+/+}$ cells, we hypothesized that IRF2a could be targeted by viruses to establish infection. To test this, we first sought to determine the interaction between IRF2a and SVCV viral proteins in the HEK293 cells. The results showed that IRF2a was immunoprecipitated with SVCV-P protein but not SVCV-N protein (Fig. 4A and B), indicating that IRF2a bound to the SVCV-P protein. In addition, we found that IRF2a did not interact with IRF1 (Fig. 4A). Next, we mapped the structural domains of IRF2a and SVCV-P responsible for the protein interaction. The N-terminal domain (1 to 101 aa, PN), central domain (101 to 187 aa, PCD), and C-terminal domain (187 to 309 aa, PC) of SVCV-P were truncated to construct mutants with an MYC-tag. For IRF2a, we generated two mutants with a GFP-tag, GFP-DN lacking the N-terminal DBD and GFP-DC lacking the C-terminal IAD. We found that GFP-DN but not GFP-DC was immunoprecipitated with MYC-SVCV-P (Fig. 4C). Further analysis revealed that FLAG-DN bound to MYC-SVCV-PC but not MYC-SVCV-PN and MYC-SVCV-PCD (Fig. 4D). Thus, it can be concluded that the IAD domain but not DBD of IRF2a bound to the C-terminal domain of SVCV-P. We also observed that in the EPC cells transfected with GFP-IRF2a, the protein levels of IRF2a steadily rose in a dose-dependent manner of SVCV-P plasmids (Fig. 4E), indicating SVCV-P could promote the accumulation of IRF2a.

It has been well documented that the transportation of active IRF2 from the cytoplasm to the nucleus is an essential step for its regulatory functions (13). Having confirmed the interaction between IRF2a and SVCV-P, we analyzed the impact of SVCV-P on the nuclear translocation of IRF2a in the EPC cells. In the absence of SVCV-P, IRF2a could be detected in both cytoplasm and nucleus and was upregulated by SVCV infection and poly(I:C) stimulation (Fig. 4F and G). The IRF2a protein levels markedly increased in the cytoplasm and nucleus of EPC cells overexpressing SVCV-P after SVCV infection (Fig. 4F) or poly(I:C) stimulation (Fig. 4G). Intriguingly, the SVCV-P protein appeared to be limited in the cytoplasm and was largely undetectable in the nucleus (Fig. 4H). These observations indicated that the coexpression of SVCV-P with IRF2a increased the IRF2a protein level in the cytoplasm and enhanced the nuclear translocation of IRF2a from the cytoplasm.

Ubiquitination is instrumental to protein degradation. Previous studies have shown that viral proteins can manipulate the ubiquitination pathway to regulate the host's

FIG 2 Legend (Continued)
PCR at 24 h (B). (C to E) The *irf2a*$^{+/+}$ and *irf2a* $^{-/-}$ caudal fin cells were infected with SVCV (MOI = 1) for 24 h. Viral titers in the culture media measured by plaque assay (C) and expression of *svcv-n* and *svcv-g* (D) and host antiviral factors, including *ifnφ1*, *ifnφ3*, *pkr*, *mx1* and *isg15* (E) ($n = 4$). (F) Analysis of principal components for the IRF2a$^{+/+}$ (WT) and IRF2a$^{-/-}$ cells treated with MEM medium (MEM) or infected with SVCV (SV). (G to I) GSEA analysis of KEGG pathways for cytokine-cytokine receptor interaction (G), mitogen-activated protein kinase (MAPK) signaling pathway (H), and TGF-beta signaling pathway (I). (J and K) Volcano plot of ISGs expressed in the IRF2a$^{+/+}$ and IRF2a$^{-/-}$ cells, including *ifnφ1*, *irf3*, *mx*, *pmsb8a*, and *pmsb9a*. Cells treated with MEM medium (J) and infected with SVCV (K). *, $P < 0.05$; **, $P < 0.01$ were considered significant.

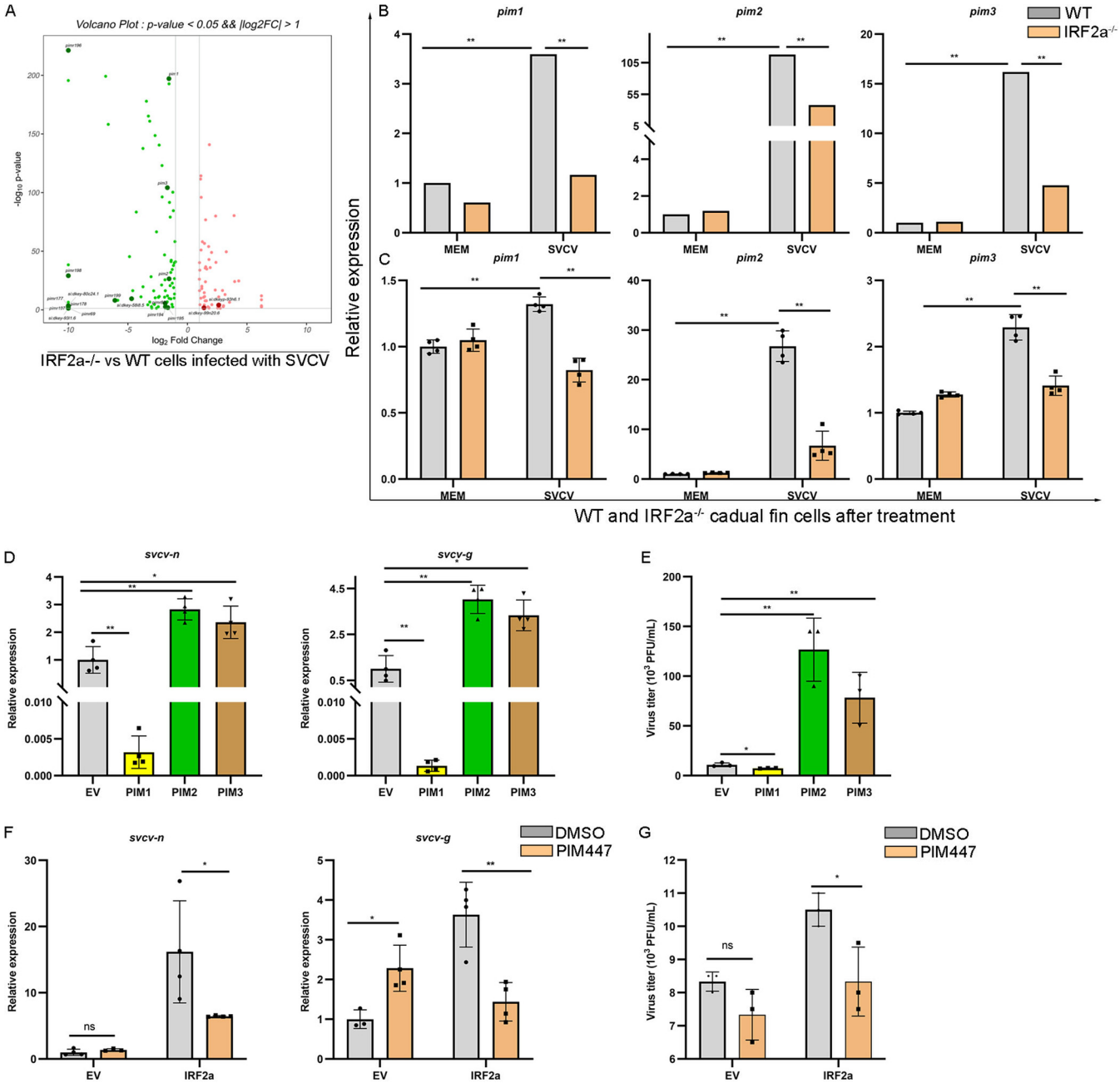

FIG 3 IRF2a downregulated *pim2* and *pim3* expression to promote SVCV replication. (A) Volcano plot of STPK (serine/threonine kinases) gene expression in the *irf2a*$^{+/+}$ (WT) and *irf2a*$^{-/-}$ cells infected with SVCV. (B) Expression levels of *pim1-3* in the RNA-seq analysis. (C) qRT-PCR validation of expression of *pim1-3* in the *irf2a*$^{+/+}$ and *irf2a*$^{-/-}$ cells infected with SVCV (n = 4). (D and E) EPC cells were transfected with *pim1*, *pim2*, or *pim3* plasmids (1 μg each). At 24 h, cells were infected with SVCV (MOI = 1). Expression of *svcv-n* and *svcv-g* (n = 4) (D) and viral titers of the culture medium collected from the above-described experiment were determined (n = 3) (E). (F) Expression of *svcv-n* and *svcv-g* (n = 4). *irf2a*$^{+/+}$ cells were transfected with empty vector (EV) and IRF2a plasmids for 24 h and treated with 5 μM PIM447or DMSO (control) for 10 h before infection with SVCV (MOI = 1). (G) Viral titers of the culture media collected from the above-described experiment were measured by plaque assay (n = 3). *, $P < 0.05$; **, $P < 0.01$ were considered significant.

antiviral response (25). To test whether SVCV-P targets the ubiquitination-proteasome pathway to inhibit the degradation of IRF2a, we expressed GFP-IRF2a and HA-tagged ubiquitin in the HEK293 cells in the presence or absence of SVCV-P. We found that SVCV-P was involved in the ubiquitination to GFP-IRF2a (Fig. 4I). Further, overexpression of SVCV-P significantly reduced the K48-linked ubiquitination of IRF2a (Fig. 4J). In contrast, the K33 and K63-linked ubiquitination had no effect, indicating that these two lysine residues were not involved in the ubiquitination-mediated degradation of

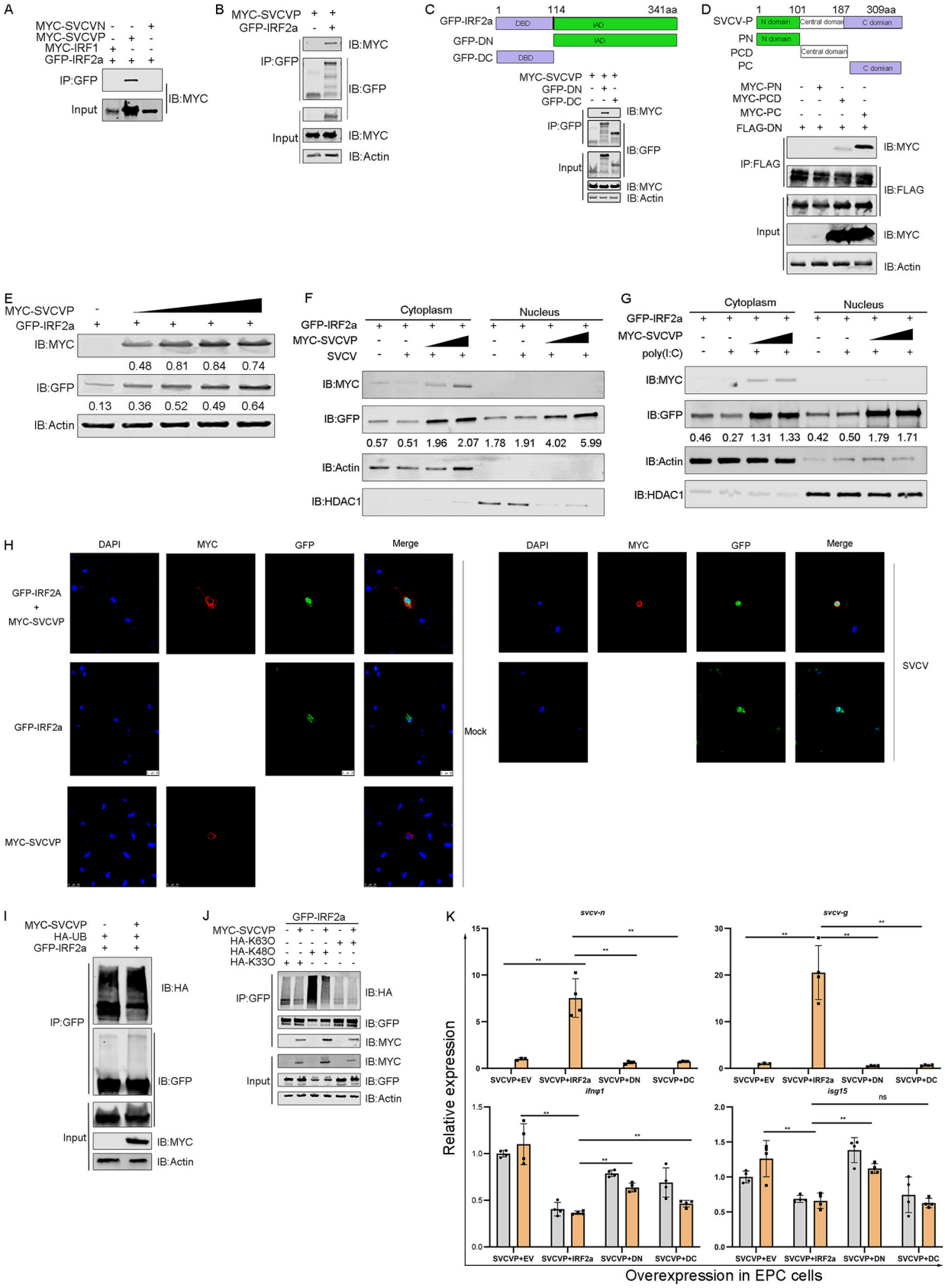

FIG 4 SVCV-P promoted IRF2a stability and nuclear translocation. (A and B) HEK293 cells were transfected with GFP-IRF2a plus MYC-IRF1, MYC-SVCVP, or MYC-SVCVN for analysis of protein interaction. (C) HEK293 cells were cotransfected with MYC-SVCVP plus GFP-IRF2a-DN or GFP-

(Continued on next page)

IRF2a (Fig. 4J). Taken together, these results illustrated that SVCV-P stabilized IRF2a via inhibition of K48-linked ubiquitination of IRF2a.

To determine whether SVCV-P negative regulation of host antiviral response is dependent on IRF2a, we coexpressed *svcv-p* with *irf2a* or *irf2a* mutants in the EPC cells and found that the transcripts of *svcv-n* and *svcv-g* significantly increased in the cells transfected with SVCV-P and IRF2a and that *ifnφ1* and *isg15* were downregulated (Fig. 4K). Such effects could be offset by cotransfection with SVCV-P and IRF2a mutants (Fig. 4K). The results suggested that SVCV-P cooperated with IRF2a to suppress the host antiviral response.

IRF2a and SVCV-P promoted the degradation of STAT1a and blocked its nuclear translocation. STAT1 is the central transcription factor orchestrating IFN-mediated antiviral response (15, 26). In teleost fish, two copies of STAT1 homologs exist and STAT1a is the dominant form to initiate IFN signaling (27). To determine whether IRF2a affects STAT1a-mediated signaling, we analyzed the interaction between IRF2a and STAT1a by immunoprecipitation in the HEK293 cells. We found that GFP-IRF2a bound to FLAG-STAT1a (Fig. 5A), and that the IAD but not DBD of IRF2a engaged in the interaction (Fig. 5B). Moreover, the interaction between IRF2a and STAT1a resulted in decreases of STAT1a protein in the EPC cells, which was partially offset by MG132 (inhibitor of proteasome pathway) but not CQ (inhibitor of the lysosomal pathway) and 3-MA (inhibitor of autophagosome pathway) (Fig. 5C). IRF2a also decreased the protein levels of total and phosphorylated STAT1a (pSTAT1a) induced by IFN-φ1 (Fig. 5D). Further, we observed that degradation of STAT1a protein was initiated by ubiquitination (Fig. 5E) because overexpression of MYC-IRF2a significantly reduced K63- but not K48-linked ubiquitination (Fig. 5F). Transcription factors translocate into the nucleus to activate transcription of target genes. After infection with SVCV or poly(I:C) stimulation, the STAT1a protein detected in the nucleus decreased in the cells cotransfected with MYC-IRF2a and STAT1a. MYC-IRF2a was also detected in the cytoplasm and nucleus (Fig. 5G and H). Confocal microscopy confirmed the nuclear translocation of IRF2a and STAT1a in response to SVCV infection (Fig. 5I and J). Taken together, our data supported that IRF2a promoted the degradation of STAT1a and pSTAT1a and inhibited its nuclear translocation.

Viruses target STAT1 to antagonize antiviral response (28, 29). We reasoned that the SVCV-P protein may inhibit STAT1-mediated signaling. To test this, we overexpressed SVCV-P and STAT1a in the HEK293 cells and performed co-immunoprecipitation (CO IP) analysis to determine their interaction. We showed that SVCV-P coimmunoprecipitated with STAT1a (Fig. 6A). Next, we asked what structural domains of the SVCV-P and STAT1a were involved in the interaction. It was evident that the C-terminal domain (187 to 309 aa, PC) of SVCV-P was responsible for binding to STAT1a (Fig. 6B). Consequently, binding of SVCV-P with STAT1a resulted in decreased protein levels of STAT1a and pSTAT1a regardless of activation by IFN-φ1 (Fig. 6C). Virus infection and poly(I:C) stimulation leads to the activation of STAT1 and subsequent nuclear translocation (30, 31). Our data showed that the SVCV-P protein could effectively block the STAT1a nuclear translocation process (Fig. 6D, lanes 6 and 8; Fig. 6E, lanes 5 and 8). Moreover, FLAG-STAT1a translocated from the cytoplasm into the nucleus in response

FIG 4 Legend (Continued)
IRF2a-DC. (D) HEK293 cells were cotransfected with FLAG-IRF2a-DN plus SVCV-P-PN, SVCV-P-PCD, or SVCV-P-PC. (E) EPC cells were cotransfected with GFP-IRF2a (1 μg) and MYC-SVCVP (0, 0.25, 0.5, and 1 μg). HEK293 cells were lysed at 24 h after transfection and cell lysates were immunoprecipitated with respective antibody-conjugated beads and immunoblotted with indicated antibodies. (F and G) EPC cells were transfected with GFP-IRF2a (1 μg) and MYC-SVCVP (0, 1, and 2 μg). After 24 h, the cells were infected with SVCV (MOI = 1) (F) or transfected with poly(I:C) (5 μg/mL) (G). Nuclear and cytosolic proteins were fractioned and analyzed by immunoblotting. Actin and HDAC1 were used as controls for the normalization of cytosolic and nuclear proteins, respectively. (H) Cellular localization of IRF2a (green) and SVCV-P (red) in the IRF2a$^{+/+}$ cells. The IRF2a$^{+/+}$ cells were transfected with GFP-IRF2a, MYC-SVCVP, or transfected with GFP-IRF2a and MYC-SVCVP. After infection with SVCV or MEM medium (mock), cells were observed under a confocal microscope. (I) HEK293 cells were transfected with MYC-SVCVP with GFP-IRF2a or HA-Ub. (J) HEK293 cells were transfected with different combinations of plasmids as indicated. HEK293 cells were lysed at 24 h after transfection and cell lysates were immunoprecipitated with respective antibody-conjugated beads and immunoblotted with indicated antibodies. (K) Expression of viral genes (*svcv-n* and *svcv-g*), *ifnφ1*, and *isg15*. EPC cells were transfected with MYC-SVCVP plus MYC-IRF2a or truncated plasmids. After 24 h, the cells were infected with SVCV (MOI = 1) (yellow bar) or incubated with MEM medium (grey bar) (n = 4). *, $P < 0.05$; **, $P < 0.01$ were considered significant.

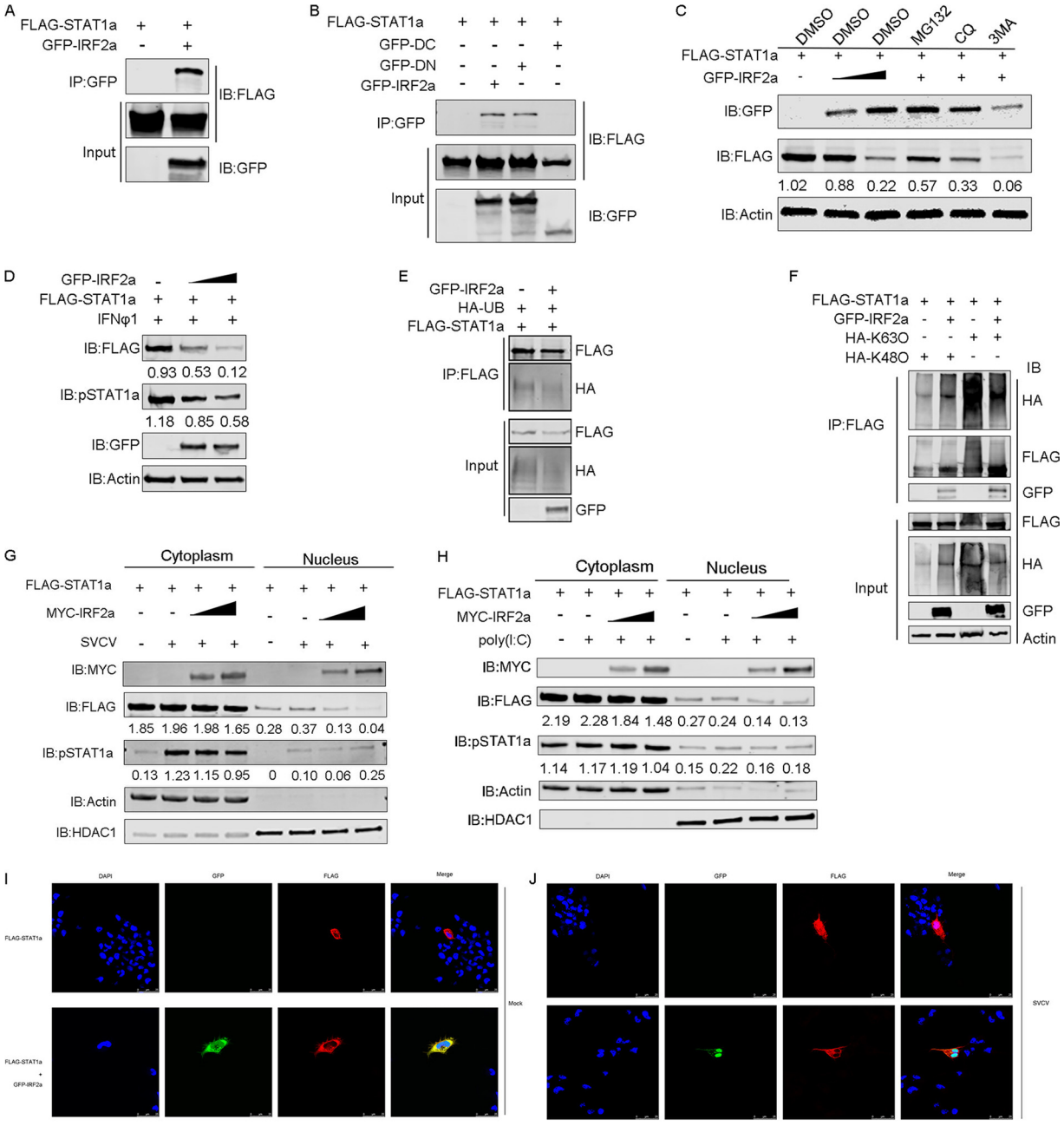

FIG 5 IRF2a targeted STAT1a to negatively regulate the JAK-STAT pathway. (A and B) IRF2a interaction with STAT1a depended on its IAD domain. HEK293 cells were cotransfected FLAG-STAT1a plus empty vector (EV), GFP-IRF2a (A), or truncated IRF2a mutants (B) for 24 h. Cells were collected for immunoprecipitation using α-GFP beads and analyzed by immunoblotting. (C and D) EPC cells were transfected with FLAG-STAT1a (1 μg) and GFP-IRF2a (0, 0.25, 1 μg). After 18 h, cells were treated with inhibitors for 6 h (C) or stimulated with IFN-φ1 protein (100 ng/mL) for 20 min (D). Cell lysates were analyzed by immunoblotting with α-actin, α-FLAG, or α-GFP. (E and F) HEK293 cells were transfected with different combinations of plasmids as indicated. At 24 h, cell lysates were immunoprecipitated with α-FLAG beads and analyzed by immunoblotting. (G and H) EPC cells were transfected with FLAG-STAT1a (1 μg) and MYC-IRF2a (0, 0.25, and 1 μg). After 24 h, cells were infected with SVCV (MOI = 1) (G) or transfected with poly(I:C) (5 μg/mL) (H). (I) Cellular localization of GFP-IRF2a (green) and FLAG-STAT1a (red). (J) The nucleus (blue) was stained with DAPI.

to SVCV infection (Fig. 6F and G). However, when cotransfected with FLAG-STAT1a and SVCV-P, FLAG-STAT1a was localized in the cytoplasm with or without SVCV infection (Fig. 6F and G), indicating that SVCV-P blocks STAT1a translocation into the nucleus.

DISCUSSION

IRF2 belongs to the IRF family and is closely related to IRF1. Its roles in regulating IFN response have not been fully understood. Previous studies have shown that IRF2

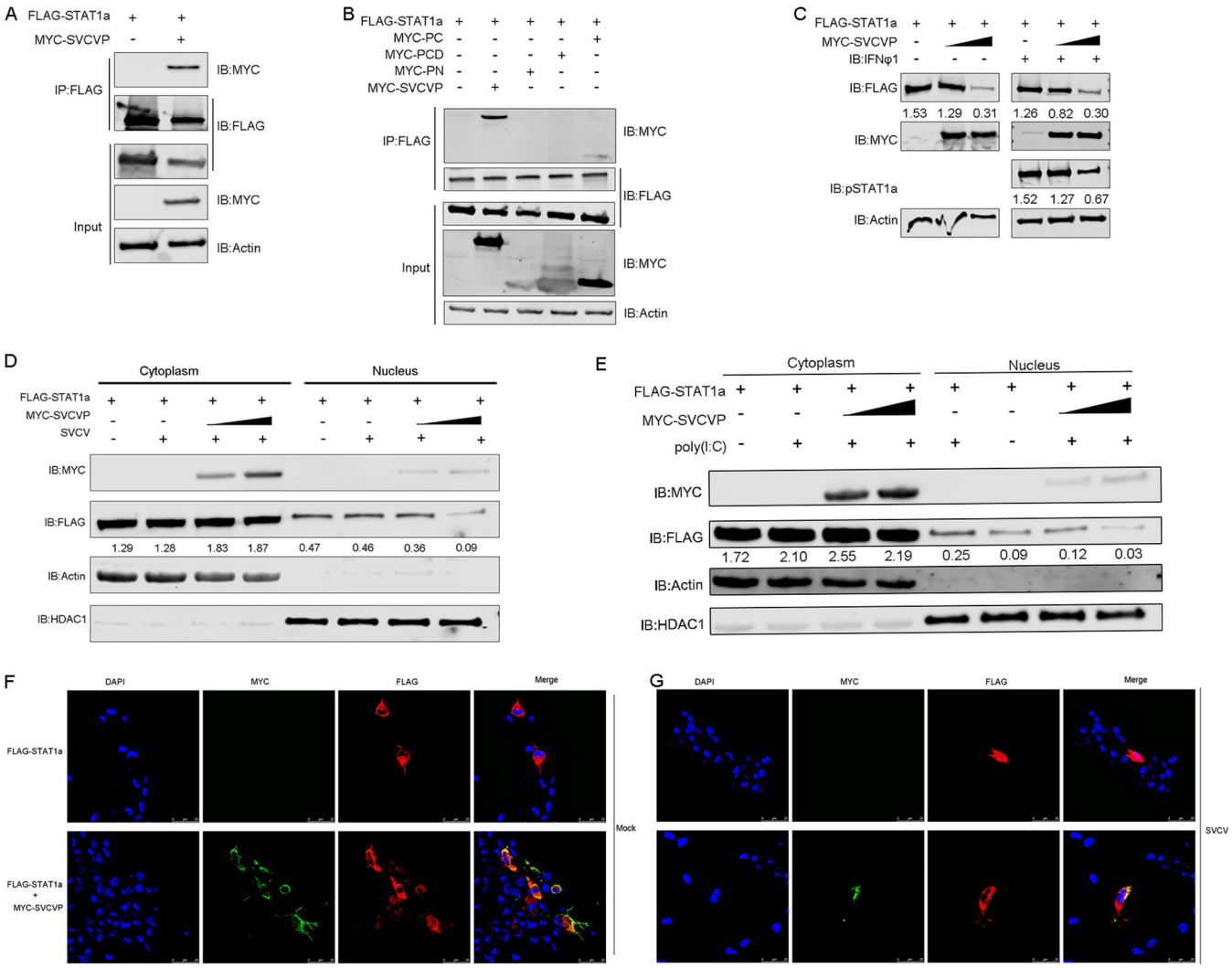

FIG 6 SVCV-P enhanced the degradation of STAT1a and blocked its nuclear translocation. (A and B) The C-terminal region of SVCV-P interacted with STAT1a. HEK293 cells were transfected with FLAG-STAT1a plus MYC-SVCVP (A) or SVCV-P mutant plasmids (MYC-SVCVP-PC, MYC-SVCVP-PCD, and MYC-SVCVP-PN) (B). At 24 h, cells were analyzed by immunoprecipitation with α-FLAG beads and immunoblotting with α-MYC. (C) EPC cells were transfected with FLAG-STAT1a (1 μg) and MYC-SVCVP (0, 0.5, and 2 μg). At 24 h, cells were treated with IFN-φ1 (100 ng/mL) for 20 min. (D and E) EPC cells were transfected with FLAG-STAT1a (1 μg) and MYC-SVCVP (0, 0.5, and 2 μg). At 24 h, cells were infected with SVCV (MOI = 1) (D) or transfected with poly(I:C) (5 μg/mL) (E). (F) Cellular localization of MYC-SVCVP (green) and FLAG-STAT1a (red). (G) The nucleus (blue) was stained with DAPI.

inhibits host IFN response by competing with IRF1 for the binding sites in the promoters of ISGs (32). Knockdown of *irf2* expression attenuates IFN signaling in zebrafish embryos (33). However, some studies have shown that IRF2 promotes infection of the West Nile virus in A172 cells and protects mice from a lethal challenge (12). In addition, IRF2-deficient mice exhibit increased mortality caused by infection with the lymphocytic choriomeningitis virus (10). Zebrafish possess two copies of the *irf2* gene, namely, *irf2a* and *irf2b*. In this study, we show that overexpression of *irf2a* decreased the promoter activity of *ifnφ1* and *ifnφ3* genes as well as the transcript levels of *ifnφ1* and *mx* (Fig. 1). Such inhibitory effects could be rescued in the *irf2a*$^{-/-}$ cells (Fig. 2). Moreover, IRF2a was shown to be indispensable for SVCV replication (Fig. 1 and 2). Our results support the notion that IRF2a is a negative regulator of IFN production.

PIM kinases are oncogenic serine/threonine kinases and are associated with hematological malignancies and solid cancers in humans (34). The PIM family consists of three members, PIM1-3. Recent studies have shown that they serve as provirus factors to promote viral infections (24, 35–37). PIM kinases activate the transcription of host factors to favor viral protein synthesis and virus entry (38). The expression of *pim* genes

is governed by the JAK-STAT and NF-κB pathways and their activities are primarily regulated at the transcriptional and translational levels (34). In our transcriptomic analysis, all three *pim* genes were downregulated in the IRF2a$^{-/-}$ cells relative to the wild-type cells following SVCV infection (Fig. 3A to C). Moreover, we found that overexpression of *pim2* and *pim3* elevated SVCV titers in the EPC cells (Fig. 3D and E), in agreement with recent findings that the PIM kinases promote virus entry and replication (35, 37–39). Furthermore, IRF2a-enhanced virus replication could be inhibited by PIM447, the inhibitor for the pan-PIM kinases (Fig. 3F and G), suggesting that IRF2a may target PIM kinases to regulate host antiviral response.

Activation of transcription factors is mainly regulated at the posttranslational level. Phosphorylation of IRFs and STATs is also an essential step for initiating IFN-mediated responses. Emerging evidence indicates that ubiquitination plays a vital role in the regulation of the activities of IRFs and STATs. For instance, ring-b-boxcoiled-coil protein interacting with protein kinase C-1, an E3 ubiquitin ligase, can degrade IRF3 via ubiquitination, resulting in suppression of Sendai virus-triggered production of type I IFNs (40). IRF3 and IRF7 can be modified by E3 ubiquitin ligase (RAUL) via K48-linked polyubiquitination to restrain type I IFN secretion (41). However, studies on the ubiquitination of IRF2 are limited. It has been shown that IRF2 can be ubiquitinated by mouse double minute 2 (Mdm2), but how this ubiquitination process affects IRF2 functions has not been investigated (42). Interestingly, we found that K48-linked ubiquitination of IRF2a was impaired by SVCV phosphoprotein, hence promoting IRF2a stability and accumulation (Fig. 4E and F). These results may partly explain why IRF2a inhibited the transcription of IRF1 and IRF7 induced by SVCV (Fig. 1F). Our study also demonstrates that IRF2a destabilized STAT1a and inhibited its activity by weakening K63-linked ubiquitination (Fig. 5F). Activation of STAT1 is regulated by polyubiquitination, which relies on E3 ubiquitin ligases such as ring finger protein 2 (RNF2), RNF220 and natural killer lytic-associated molecule (NKLAM) and is essential for JAK/STAT signal transduction (43, 44). IRF2a is not an E3 ubiquitin ligase. However, as a transcription factor, IRF2a can regulate the expression of genes involved in posttranslational modifications (unpublished data), suggesting that it cooperates with ubiquitin ligases to control protein metabolism. Viral phosphoprotein is known to interact with STAT1 to antagonize the JAK-STAT pathway (19, 45). This is supported by our observation that SVCV-P interacted with both STAT1a and IRF2a (Fig. 4D and 6B). We showed that the C-terminal region (187 to 309 aa) was required for the interaction with the IAD domain of IRF2a and STAT1a, contrasting with the previous study where the central domain (101 to 187 aa) of SVCV-P was shown to negatively regulate host IFN production (46). This may be due to the diverse functions of the different domains of SVCV-P. The central domain of the phosphoprotein of *Rhabdovirus* is responsible for homodimerization, leading to phosphorylation (46, 47), while the C-terminal region binds to large polymerase and nucleocapsid protein for viral RNA synthesis (48, 49).

In summary, we reported here that overexpression of zebrafish IRF2a negatively regulated IFN production and facilitated viral replication. The *irf2a* knockout zebrafish and derived primary cells displayed increased resistance to SVCV infection. Transcriptomic analysis revealed that the IFN-stimulated genes (ISGs), including *pkz*, *mxa*, *mxb*, and *smad3*, were elevated in the *irf2a*$^{-/-}$ cells compared to the wild-type cells. We found that the expression of *pim* family kinases (*pim2* and *pim3*) was suppressed in the *irf2a*$^{-/-}$ cells. Importantly, the accumulation of IRF2a was enhanced by SVCV-P, and this process could be inhibited via K48-linked polyubiquitination. Both IRF2a and SVCV-P are involved in the degradation of STAT1a to impede IFN-mediated signaling. We propose a model to demonstrate that IRF2a is a negative regulator of IFN response and is a prime target for the virus to evade host antiviral defense (Fig. 7).

MATERIALS AND METHODS

Fish. Wild type (strain AB) and *irf2a*$^{+/-}$ knockout (number ZKO733) zebrafish were generated by the China Zebrafish Resource Center (50). Fish were checked by PCR to ensure that the experimental fish were free of common cyprinid viruses such as spring viremia of carp virus (SVCV), grass carp reovirus,

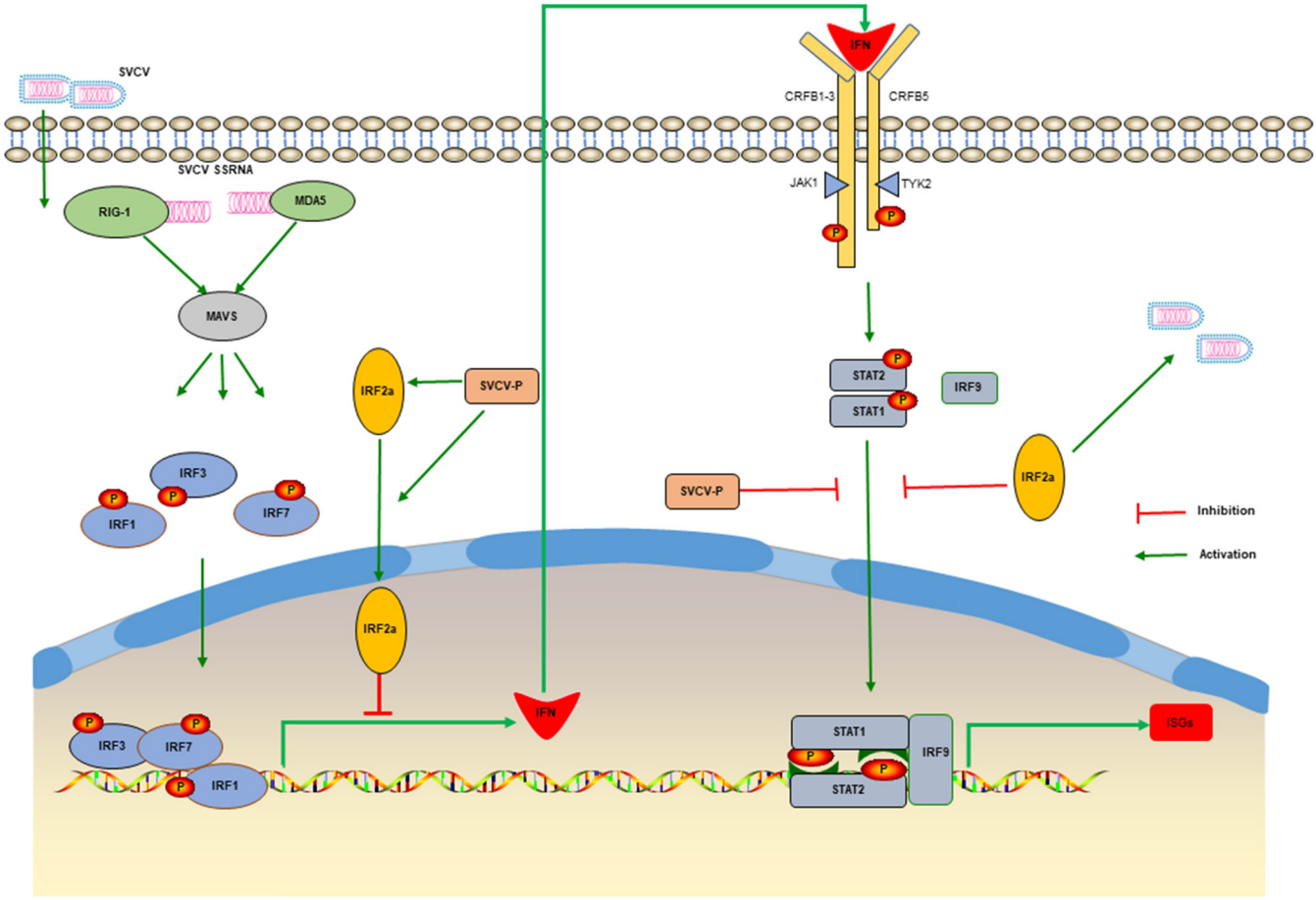

FIG 7 Proposed model for the regulatory function of IRF2a. IRF2a negatively regulated innate antiviral immunity in zebrafish. IRF2a deficiency promoted host IFN response and antiviral resistance. This was partly achieved by the enhancement of IRF2a nuclear translocation and protein stability via interacting with viral phosphoprotein. IRF2a cooperated with viral phosphoprotein to destabilize STAT1a and block its translocation into the nucleus.

and cyprinid herpesvirus, and maintained in an indoor aquarium at 28 ± 1°C with aerated circulating water. The *irf2a*$^{-/-}$ knockout zebrafish were obtained by cross-breeding. Fish were anesthetized with MS-222 (100 mg/L, Sigma-Aldrich) before experimental procedures. All experiments were conducted under the guidelines of Shanghai Ocean University on the use of animals for research (SHOU-DW-2019-003).

Plasmids and reagents. The following plasmids of zebrafish genes are listed in Table 1. The pGL3-*ifnφ1*pro and pGL3-*ifnφ3*pro were constructed as previously described (51), ISREpro (number E4141), and pRL-TK (number E2241) purchased from Promega. Hemagglutinin (HA)-tagged ubiquitin (HA-Ub)

TABLE 1 Plasmid information used in this study

Plasmid	GenBank accession no.
pEGFP-N1-IRF2a	NM_001326712
pEGFP-N1-IRF2a-DN	NM_001326712
pEGFP-N1-IRF2a-DC	NM_001326712
pcDNA3.1-FLAG-IRF2a-DN	NM_001326712
pcDNA3.1-MYC-IRF7	NM_200677.2
pcDNA3.1-FLAG-STAT1a	NM_131480
pcDNA3.1-MYC-SVCVP-PCD	NP_116745
pcDNA3.1-PIM1	NM_001077391.1
pcDNA3.1-PIM2	NM_131539.2
pcDNA3.1-PIM3	NM_001034978.2
pcDNA3.1-MYC-IRF1	NM_205747.1
pcDNA3.1-SVCVP	NP_116745
pcDNA3.1-MYC-SVCVP-PN	NP_116745
pcDNA3.1-MYC-SVCVP-PC	NP_116745

plasmid and mutants (HA-K33O, HA-K48O, and HA-K63O) were purchased from HedgehogBio (numbers HH-gene-099, HH-gene-121, HH-gene-122, and HH-gene-123).

Antibodies used in the study included α-Flag (number M1403-2, Huabio), α-HA (number 0906-1, Huabio), α-MYC (number EM31105 and number R1208-1, Huabio), and α-Actin (number ET1702-52, Huabio), rabbit α-GFP (number 300943, Zen-bio) (1:1000, vol/vol), mouse α-GFP (number M20004, Abmart), rabbit α-HDAC1 (number T40107, Abmart), α-MYC beads (number M20012, Abmart), α-GFP beads (number M20015, Abmart) and α-MYC beads (number M20018, Abmart), goat α-mouse IgG (number 926-32210, LI-COR), goat α-rabbit IgG (number 926-32211, LI-COR), Alexa Fluor 594-conjugated α-rabbit IgG (Cell Signaling) and Alexa Fluor 594-conjugated α-mouse IgG (Zenbio). The jetOPTIMUS (number 101000006) for transfection was purchased from Polyplus. The Minute™ Cytoplasmic and Nuclear Fractionation kit was purchased from Invent (number SC-003) for the extraction of nuclear and cytosolic proteins. Poly(I·C) (number P1530) and PIM447 (number S7985) were purchased from Merck and Selleckchem, respectively.

Cells, viruses, and infection. The HEK293 (ATCC, number CRL-3216) and *Epithelioma papulosum cyprini* (EPC) (ATCC, number CRL-2872) cell lines were cultured in Dulbecco's modified Eagle's medium (DMEM) containing 10% fetal bovine serum (FBS) and 1% penicillin-streptomycin in a humidified 5% CO_2 incubator at 37°C and 28°C, respectively. Caudal fin cells were generated from *irf2a*$^{+/+}$ and *irf2a*$^{-/-}$ adult zebrafish and maintained in DMEM/F12 supplemented with 10% FBS in a humidified 5% CO_2 incubator at 28°C. The caudal fin was sampled from an adult zebrafish and washed several times with sterile PBS buffer containing 1% penicillin-streptomycin. After cutting into small pieces, the diced fin tissue was placed in a 15 mL tube, shaken vigorously for 5 min, filtered through a nylon filter (70 μM, Millipore), and extensively washed with PBS. The fin tissues were then transferred into a 25 cm^2 flask containing DMEM/F12 medium supplemented with 20% FBS and cultured in a humidified 5% CO_2 incubator at 28°C. After 20 passages, the cells were applied for the following experiments.

Spring viremia of carp virus was prepared in the EPC cells and titers were determined as 50% tissue culture-infective dose ($TCID_{50}$) (52). For the challenge experiment, zebrafish larvae at 5 d postfertilization (dpf) were infected with 3×10^7 $TCID_{50}$/fish SVCV by immersion in Petri-dishes at 22°C for 12 h and the solution was replaced by distilled water. After an additional 24 h, larvae were sampled for qRT-PCR analysis. At 44 h, mortalities were recorded.

Plaque formation assay. EPC cells were seeded in 12-well plates. When the cells grew to confluence, the supernatant from SVCV-infected cells was diluted 10-fold and then added into the monolayer. After 1 h, the medium was removed and replaced with fresh DMEM medium containing 2% FBS and 1.5% carboxymethyl cellulose (Sigma-Aldrich) at 22°C. When the cytopathic effect (CPE) appeared (between 48 and 72 h), the cells were fixed with 4% polyformaldehyde for 15 min and stained with 1% crystal violet for 1 h. After washing with water, visible plaques were counted, and viral titers were determined.

RNA-seq. RNA was extracted from the primary cells derived from *irf2a*$^{+/+}$ and *irf2a*$^{-/-}$ zebrafish using TRIzol reagent (number 15596026, ThermoFisher) and used for deep sequencing using an Illumina HiSeq X 10 platform. Reads were mapped to the zebrafish genome (version GRCz11) and analyzed using the DESeq package. $P < 0.05$ and a fold change >2 or a fold change <0.5 were set as the threshold for differential expression with significance. Hierarchical cluster analysis of differentially expressed genes (DEGs) was performed to determine the expression patterns of genes in different groups. Principal component analysis (PCA) was performed using the function plotPCA in the DESeq package. Gene ontology (GO) enrichment and KEGG pathway enrichment analysis of DEGs were performed using the R program based on the hypergeometric distribution.

Luciferase reporter assay. In a 24-well plate, EPC cells were cultured to 80 to 90% confluence and transfected with a mixture of 250 ng of luciferase reporter (firefly luciferase) plasmid and 25 ng of pRL-TK (Renilla luciferase plasmid) plus target plasmids. After 24 h, the cells were transfected with poly(I:C) or infected with SVCV and cultured for an additional 24 h. Luciferase activity was measured using a Dual-Luciferase Reporter Assay System kit according to the manufacturer's protocol. Renilla luciferase was used as an internal control to normalize firefly luciferase activity.

Quantitative real-time PCR. Total RNA was extracted using TRIzol reagent following the manufacturer's instructions and reverse-transcribed using the HifairII 1st Strand cDNA Synthesis SuperMix (number 11123ES10, Yeasen). qRT-PCR was performed using Hieff UNICON Power qPCR SYBR Green Master Mix (number 11195ES03, Yeasen) and run on the LightCycler 480 Real-Time System (Roche). Primers for qRT-PCR are listed in Table 2. qRT-PCR was run in triplicate and repeated at least three times. *Ef1*α and *β-actin* were used as references to normalize the expression levels of target genes in zebrafish cells and EPC cells, respectively.

Immunoprecipitation and Western blotting. Cells were lysed with RIPA buffer (number P0013C, Beyotime) and immunoprecipitated with proteinA/G resin (number 36403ES03, Yeasen) and then with antibody-conjugated beads. Cell lysates or immunoprecipitated proteins were electrophoresed in a 12% SDS-PAGE gel and transferred to a polyvinylidene fluoride (PVDF) membrane (Millipore). The membrane was blocked with 5% skim milk in TBS buffer and incubated with the primary and secondary antibodies. Protein bands were visualized using an Odyssey CLx Imaging System (LI-COR).

Immunofluorescent microscopy. In a 6-well plate, cells were cultured to 80 to 90% confluence and transfected with plasmids. After 24 h, cells were washed twice with PBS buffer and fixed with 4% polyformaldehyde solution at room temperature for 10 min, permeabilized with PBS buffer containing 0.1% Triton X-100 for 5 min, washed three times with PBS buffer, and blocked with PBS containing 5% bovine serum albumin (BSA) for 1 h. The cells were then incubated with the primary antibody at 4°C overnight and incubated with Alexa Fluor 594-conjugated α-rabbit IgG and Alexa Fluor 594-conjugated α-mouse IgG for 1 h. After washing three times, the cells were incubated with DAPI solution (Yeasen) for 5 min

TABLE 2 Primer sequences used in this study

Primer name	Sequence (5′ to 3′)
ef1a-F	CTGGAGGCCAGCTCAAACAT
ef1a-R	ATCAAGAAGAGTAGTACCGCTAGCATTAC
ifnφ1-ZF-F	TGGAGGACCAGGTGAAGTT
ifnφ1-ZF-R	ATTGACCCTTGCGTTGCTT
isg15-ZF-F	CTGACTGTAAAACTGCTTGGCGG
isg15-ZF-R	CGTTGGCGTCCACATCATAAG
mx1-ZF-F	GACCGTCTCTGATGTGGTTA
mx1-ZF-R	GCATGCTTTAGACTCTGGCT
pkr-ZF-F	AGGTGCTGAAGGCTGTGGAGTA
pkr-ZF-R	TTCCCGTCCTTTTAGTTCGTTC
ifnφ3-ZF-F	GAGGATCAGGTTACTGGTGT
ifnφ3-ZF-R	GTTCATGATGCATGTGCTGTA
pim1-ZF-F	TGCGAACCGGCGATCTGAAG
pim1-ZF-R	ATCGACCGTGGTAGCGGTGA
pim2-ZF-F	GGCCATCGAGGCATCATCCG
pim2-ZF-R	GCTTGAGGAACCTCCGTGCAA
pim3-ZF-F	GTGCGGAGACATCCCGTTCG
pim3-ZF-R	CAACGTGGGCCGGTCTGAAG
apol-ZF-F	GGCGTGACCAGTGGTGTCAAT
apol-ZF-R	GCCTTCCTGCTGCAGACACA
mda5a-ZF-F	CCTGACGAGGAAGGCAACATTACA
mda5b-ZF-R	AACTGGCTTGGACTCCCACTTCAT
stat1b-ZF-F	TCGGAGGACCACCTAATGCGT
stat1b-ZF-R	GGCTGCCTCTCCACCACAAG
β-actin-EPC-F	CACTGTGCCCATCTACGAG
β-actin-EPC-R	CCATCTCCTGCTCGAAGTC
isg15-EPC-F	CAGCCTTGAGGATGATTCCAG
isg15-EPC-R	TGCCGTTGTAAATCAGTCG
ifn-EPC-F	ATGAAAACTCAAATGTGGACGTA
ifn-EPC-R	GATAGTTTCCACCCATTTCCTTAA
svcv-n-F	TCTGCCAAATCACCATACTCA
svcv-n-R	CTGTCTTGCGTTCAGTGCTC
svcv-g-F	ATCATTCAAAGGATTGCATCAG
svcv-g-R	CATATGGCTCTAAATGAACAGAA

and then washed three more times with PBS buffer. The cells were photographed under a confocal laser scanning microscope (Leica SP8).

Statistical information. Data were analyzed using a two-tailed Student's *t* test with the Prism 9 software (GraphPad), to determine differences at the 5% and 1% levels of significance.

Data availability. RNA-seq data have been deposited in the NCBI BioProject database under accession number PRJNA811714.

ACKNOWLEDGMENTS

This work is supported by the National Natural Science Foundation of China (Grant No. 32030112 and U21A20268). We thank Shanghai OE biological technology CO., LTD (Shanghai, China) for providing transcriptome services and the China Zebrafish Resource Center (CZRC) for providing the IRF2a knockout zebrafish.

We declare no conflict of interest.

REFERENCES

1. Ikushima H, Negishi H, Taniguchi T. 2013. The IRF family transcription factors at the interface of innate and adaptive immune responses. Cold Spring Harbor Symp Quant Biol 78:105–116. https://doi.org/10.1101/sqb.2013.78.020321.
2. Clark TC, Boudinot P, Collet B. 2021. Evolution of the IRF family in salmonids. Genes 12:238. https://doi.org/10.3390/genes12020238.
3. Negishi H, Taniguchi T, Yanai H. 2018. The interferon (IFN) class of cytokines and the IFN regulatory factor (IRF) transcription factor family. Cold Spring Harb Perspect Biol 10:a028423. https://doi.org/10.1101/cshperspect.a028423.
4. Tamura T, Yanai H, Savitsky D, Taniguchi T. 2008. The IRF family transcription factors in immunity and oncogenesis. Annu Rev Immunol 26:535–584. https://doi.org/10.1146/annurev.immunol.26.021607.090400.
5. Feng H, Zhang Y-B, Gui J-F, Lemon SM, Yamane D. 2021. Interferon regulatory factor 1 (IRF1) and anti-pathogen innate immune responses. PLoS Pathog 17:e1009220. https://doi.org/10.1371/journal.ppat.1009220.
6. Hatesuer B, Hoang HTT, Riese P, Trittel S, Gerhauser I, Elbahesh H, Geffers R, Wilk E, Schughart K. 2017. Deletion of Irf3 and Irf7 genes in mice results in altered interferon pathway activation and granulocyte-

dominated inflammatory responses to influenza A infection. J Innate Immun 9:145–161. https://doi.org/10.1159/000450705.
7. Panda D, Gjinaj E, Bachu M, Squire E, Novatt H, Ozato K, Rabin RL. 2019. IRF1 maintains optimal constitutive expression of antiviral genes and regulates the early antiviral response. Front Immunol 10:1019. https://doi.org/10.3389/fimmu.2019.01019.
8. Irving AT, Zhang Q, Kong P-S, Luko K, Rozario P, Wen M, Zhu F, Zhou P, Ng JHJ, Sobota RM, Wang L-F. 2020. Interferon regulatory factors IRF1 and IRF7 directly regulate gene expression in bats in response to viral infection. Cell Rep 33:108345. https://doi.org/10.1016/j.celrep.2020.108345.
9. Carlin AF, Plummer EM, Vizcarra EA, Sheets N, Joo Y, Tang W, Day J, Greenbaum J, Glass CK, Diamond MS, Shresta S. 2017. An IRF-3-, IRF-5-, and IRF-7-independent pathway of dengue viral resistance utilizes IRF-1 to stimulate type I and II interferon responses. Cell Rep 21:1600–1612. https://doi.org/10.1016/j.celrep.2017.10.054.
10. Matsuyama T, Kimura T, Kitagawa M, Pfeffer K, Kawakami T, Watanabe N, Kündig TM, Amakawa R, Kishihara K, Wakeham A, Potter J, Furlonger CL, Narendran A, Suzuki H, Ohashi PS, Paige CJ, Taniguchi T, Mak TW. 1993. Targeted disruption of IRF-1 or IRF-2 results in abnormal type I IFN gene induction and aberrant lymphocyte development. Cell 75:83–97. https://doi.org/10.1016/S0092-8674(05)80086-8.
11. Yeo KL, Ng ML. 2008. Interferon regulatory factor 2 (IRF2) regulates molecular pathogenesis of west nile virus (WNV) infection in brain cells. Int J Infect Dis 12:e295. https://doi.org/10.1016/j.ijid.2008.05.790.
12. Li MM, Bozzacco L, Hoffmann HH, Breton G, Loschko J, Xiao JW, Monette S, Rice CM, MacDonald MR. 2016. Interferon regulatory factor 2 protects mice from lethal viral neuroinvasion. J Exp Med 213:2931–2947. https://doi.org/10.1084/jem.20160303.
13. Han K-J, Jiang L, Shu H-B. 2008. Regulation of IRF2 transcriptional activity by its sumoylation. Biochem Biophys Res Commun 372:772–778. https://doi.org/10.1016/j.bbrc.2008.05.103.
14. Chae M, Kim K, Park S-M, Jang I-S, Seo T, Kim D-M, Kim I-C, Lee J-H, Park J. 2008. IRF-2 regulates NF-κB activity by modulating the subcellular localization of NF-κB. Biochem Biophys Res Commun 370:519–524. https://doi.org/10.1016/j.bbrc.2008.03.136.
15. Rouyez M-C, Lestingi M, Charon M, Fichelson S, Buzyn A, Dusanter-Fourt I. 2005. IFN regulatory factor-2 cooperates with STAT1 to regulate transporter associated with antigen processing-1 promoter activity. J Immunol 174:3948–3958. https://doi.org/10.4049/jimmunol.174.7.3948.
16. Li A, Wang W, Wang Y, Chen K, Xiao F, Hu D, Hui L, Liu W, Feng Y, Li G, Tan Q, Liu Y, Wu K, Wu J. 2020. NS5 conservative site is required for zika virus to restrict the RIG-I signaling. Front Immunol 11:51. https://doi.org/10.3389/fimmu.2020.00051.
17. Gack MU, Albrecht RA, Urano T, Inn KS, Huang IC, Carnero E, Farzan M, Inoue S, Jung JU, Garcia-Sastre A. 2009. Influenza A virus NS1 targets the ubiquitin ligase TRIM25 to evade recognition by the host viral RNA sensor RIG-I. Cell Host Microbe 5:439–449. https://doi.org/10.1016/j.chom.2009.04.006.
18. Vidy A, El Bougrini J, Chelbi-Alix MK, Blondel D. 2007. The nucleocytoplasmic rabies virus P protein counteracts interferon signaling by inhibiting both nuclear accumulation and DNA binding of STAT1. J Virol 81:4255–4263. https://doi.org/10.1128/JVI.01930-06.
19. Hossain MA, Larrous F, Rawlinson SM, Zhan J, Sethi A, Ibrahim Y, Aloi M, Lieu KG, Mok Y-F, Griffin MDW, Ito N, Ose T, Bourhy H, Moseley GW, Gooley PR. 2019. Structural elucidation of viral antagonism of innate immunity at the STAT1 interface. Cell Rep 29:1934–1945.e8. https://doi.org/10.1016/j.celrep.2019.10.020.
20. Li S, Lu L-F, Wang Z-X, Lu X-B, Chen D-D, Nie P, Zhang Y-A, Williams B. 2016. The P protein of spring viremia of carp virus negatively regulates the fish interferon response by inhibiting the kinase activity of TANK-binding kinase 1. J Virol 90:10728–10737. https://doi.org/10.1128/JVI.01381-16.
21. Lu L-F, Li S, Lu X-B, LaPatra SE, Zhang N, Zhang X-J, Chen D-D, Nie P, Zhang Y-A. 2016. Spring viremia of carp virus N protein suppresses fish IFNφ1 production by targeting the mitochondrial antiviral signaling protein. J Immunol 196:3744–3753. https://doi.org/10.4049/jimmunol.1502038.
22. Levraud J-P, Jouneau L, Briolat V, Laghi V, Boudinot P. 2019. IFN-stimulated genes in zebrafish and humans define an ancient arsenal of antiviral immunity. J Immunol 203:3361–3373. https://doi.org/10.4049/jimmunol.1900804.
23. Canova MJ, Molle V. 2014. Bacterial serine/threonine protein kinases in host-pathogen interactions. J Biol Chem 289:9473–9479. https://doi.org/10.1074/jbc.R113.529917.
24. Pereiro P, Álvarez-Rodríguez M, Valenzuela-Muñoz V, Gallardo-Escárate C, Figueras A, Novoa B. 2020. RNA-seq analysis reveals that spring viraemia of carp virus induces a broad spectrum of PIM kinases in zebrafish kidney that promote viral entry. Fish Shellfish Immunol 99:86–98. https://doi.org/10.1016/j.fsi.2020.01.055.
25. Feng P, Li S, Lu L-F, Liu S-B, Zhang C, Li Z-C, Zhou X-Y, Zhang Y-A. 2019. Spring viraemia of carp virus modulates p53 expression using two distinct mechanisms. PLoS Pathog 15:e1007695. https://doi.org/10.1371/journal.ppat.1007695.
26. Cuesta N, Nhu QM, Zudaire E, Polumuri S, Cuttitta F, Vogel SN. 2007. IFN regulatory factor-2 regulates macrophage apoptosis through a STAT1/3- and Caspase-1-dependent mechanism. J Immunol 178:3602–3611. https://doi.org/10.4049/jimmunol.178.6.3602.
27. Gan Z, Chen SN, Huang B, Zou J, Nie P. 2020. Fish type I and type II interferons: composition, receptor usage, production and function. Rev Aquacult 12:773–804. https://doi.org/10.1111/raq.12349.
28. Whelan SPJ, Harrison AR, Lieu KG, Larrous F, Ito N, Bourhy H, Moseley GW. 2020. Lyssavirus P-protein selectively targets STAT3-STAT1 heterodimers to modulate cytokine signalling. PLoS Pathog 16:e1008767. https://doi.org/10.1371/journal.ppat.1008767.
29. Wiltzer L, Okada K, Yamaoka S, Larrous F, Kuusisto HV, Sugiyama M, Blondel D, Bourhy H, Jans DA, Ito N, Moseley GW. 2014. Interaction of rabies virus P-protein with STAT proteins is critical to lethal rabies disease. J Infect Dis 209:1744–1753. https://doi.org/10.1093/infdis/jit829.
30. Vidy A, Chelbi-Alix M, Blondel D. 2005. Rabies virus P protein interacts with STAT1 and inhibits interferon signal transduction pathways. J Virol 79:14411–14420. https://doi.org/10.1128/JVI.79.22.14411-14420.2005.
31. Mu J, Fang Y, Yang Q, Shu T, Wang A, Huang M, Jin L, Deng F, Qiu Y, Zhou X. 2020. SARS-CoV-2 N protein antagonizes type I interferon signaling by suppressing phosphorylation and nuclear translocation of STAT1 and STAT2. Cell Discov 6:e1008767. https://doi.org/10.1038/s41421-020-00208-3.
32. Harada H, Fujita T, Miyamoto M, Kimura Y, Maruyama M, Furia A, Miyata T, Taniguchi T. 1989. Structurally similar but functionally distinct factors, IRF-1 and IRF-2, bind to the same regulatory elements of IFN and IFN-inducible genes. Cell 58:729–739. https://doi.org/10.1016/0092-8674(89)90107-4.
33. Li Y, Esain V, Teng L, Xu J, Kwan W, Frost IM, Yzaguirre AD, Cai X, Cortes M, Maijenburg MW, Tober J, Dzierzak E, Orkin SH, Tan K, North TE, Speck NA. 2014. Inflammatory signaling regulates embryonic hematopoietic stem and progenitor cell production. Genes Dev 28:2597–2612. https://doi.org/10.1101/gad.253302.114.
34. Brault L, Gasser C, Bracher F, Huber K, Knapp S, Schwaller J. 2010. PIM serine/threonine kinases in the pathogenesis and therapy of hematologic malignancies and solid cancers. Haematologica 95:1004–1015. https://doi.org/10.3324/haematol.2009.017079.
35. Miyakawa K, Matsunaga S, Yokoyama M, Nomaguchi M, Kimura Y, Nishi M, Kimura H, Sato H, Hirano H, Tamura T, Akari H, Miura T, Adachi A, Sawasaki T, Yamamoto N, Ryo A. 2019. PIM kinases facilitate lentiviral evasion from SAMHD1 restriction via Vpx phosphorylation. Nat Commun 10:1844. https://doi.org/10.1038/s41467-019-09867-7.
36. Zhou F, Wan Q, Lu J, Chen Y, Lu G, He M-L. 2019. Pim1 impacts enterovirus A71 replication and represents a potential target in antiviral therapy. iScience 19:715–727. https://doi.org/10.1016/j.isci.2019.08.008.
37. Zhou F, Wan Q, Chen Y, Chen S, He M-l. 2021. PIM1 kinase facilitates Zika virus replication by suppressing host cells' natural immunity. Signal Transduct Target Ther 6:207. https://doi.org/10.1038/s41392-021-00539-x.
38. Park C, Min S, Park E-M, Lim Y-S, Kang S, Suzuki T, Shin E-C, Hwang SB, Diamond MS. 2015. Pim kinase interacts with nonstructural 5A protein and regulates hepatitis C virus entry. J Virol 89:10073–10086. https://doi.org/10.1128/JVI.01707-15.
39. Früh K, Cheng F, Weidner-Glunde M, Varjosalo M, Rainio E-M, Lehtonen A, Schulz TF, Koskinen PJ, Taipale J, Ojala PM. 2009. KSHV reactivation from latency requires Pim-1 and Pim-3 kinases to inactivate the latency-associated nuclear antigen LANA. PLoS Pathog 5:e1000324. https://doi.org/10.1371/journal.ppat.1000324.
40. Zhang M, Tian Y, Wang R-P, Gao D, Zhang Y, Diao F-C, Chen D-Y, Zhai Z-H, Shu H-B. 2008. Negative feedback regulation of cellular antiviral signaling by RBCK1-mediated degradation of IRF3. Cell Res 18:1096–1104. https://doi.org/10.1038/cr.2008.277.
41. Yu Y, Hayward GS. 2010. The ubiquitin E3 ligase RAUL negatively regulates type I interferon through ubiquitination of the transcription factors IRF7 and IRF3. Immunity 33:863–877. https://doi.org/10.1016/j.immuni.2010.11.027.
42. Pettersson S, Kelleher M, Pion E, Wallace M, Ball Kathryn L. 2009. Role of Mdm2 acid domain interactions in recognition and ubiquitination of the transcription factor IRF-2. Biochem J 418:575–585. https://doi.org/10.1042/BJ20082087.

43. Guo X, Ma P, Li Y, Yang Y, Wang C, Xu T, Wang H, Li C, Mao B, Qi X. 2021. RNF220 mediates K63-linked polyubiquitination of STAT1 and promotes host defense. Cell Death Differ 28:640–656. https://doi.org/10.1038/s41418-020-00609-7.
44. Lawrence DW, Kornbluth J. 2016. E3 ubiquitin ligase NKLAM ubiquitinates STAT1 and positively regulates STAT1-mediated transcriptional activity. Cell Signal 28:1833–1841. https://doi.org/10.1016/j.cellsig.2016.08.014.
45. Schnell MJ, Zhan J, Harrison AR, Portelli S, Nguyen TB, Kojima I, Zheng S, Yan F, Masatani T, Rawlinson SM, Sethi A, Ito N, Ascher DB, Moseley GW, Gooley PR. 2021. Definition of the immune evasion-replication interface of rabies virus P protein. PLoS Pathog 17:e1009729. https://doi.org/10.1371/journal.ppat.1009729.
46. Wang Z-X, Liu S-B, Guan H, Lu L-F, Tu J-G, Ouyang S, Zhang Y-A, Parrish CR. 2020. Structural and functional characterization of the phosphoprotein central domain of spring viremia of carp virus. J Virol 94:e00855. https://doi.org/10.1128/JVI.00855-20.
47. Gerard FCA, Jamin M, Blackledge M, Blondel D, Bourhis JM. 2020. Vesicular stomatitis virus phosphoprotein dimerization domain is dispensable for virus growth. J Virol 94:e01789-19. https://doi.org/10.1128/JVI.01789-19.
48. Green TJ, Luo M. 2009. Structure of the vesicular stomatitis virus nucleocapsid in complex with the nucleocapsid-binding domain of the small polymerase cofactor, *P* Proc Natl Acad Sci U S A 106:11713–11718. https://doi.org/10.1073/pnas.0903228106.
49. Jenni S, Bloyet L-M, Diaz-Avalos R, Liang B, Whelan SPJ, Grigorieff N, Harrison SC. 2020. Structure of the vesicular stomatitis virus L protein in complex with its phosphoprotein cofactor. Cell Rep 30:53–60.e5. https://doi.org/10.1016/j.celrep.2019.12.024.
50. Sun Y, Zhang B, Luo L, Shi DL, Wang H, Cui Z, Huang H, Cao Y, Shu X, Zhang W, Zhou J, Li Y, Du J, Zhao Q, Chen J, Zhong H, Zhong TP, Li L, Xiong JW, Peng J, Xiao W, Zhang J, Yao J, Yin Z, Mo X, Peng G, Zhu J, Chen Y, Zhou Y, Liu D, Pan W, Zhang Y, Ruan H, Liu F, Zhu Z, Meng A, Consortium Z. 2020. Systematic genome editing of the genes on zebrafish Chromosome 1 by CRISPR/Cas9. Genome Res 30:118–126. https://doi.org/10.1101/gr.248559.119.
51. Sun F, Zhang Y-B, Liu T-K, Shi J, Wang B, Gui J-F. 2011. Fish MITA serves as a mediator for distinct Fish IFN gene activation dependent on IRF3 or IRF7. J Immunol 187:2531–2539. https://doi.org/10.4049/jimmunol.1100642.
52. Zhang J, Wu XM, Hu YW, Chang MX. 2020. A novel transcript isoform of TBK1 negatively regulates type I IFN production by promoting proteasomal degradation of TBK1 and lysosomal degradation of IRF3. Front Immunol 11:580864. https://doi.org/10.3389/fimmu.2020.580864.